

Article

Effect of Hull and Propeller Roughness during the Assessment of Ship Fuel Consumption

Mina Tadros ^{1,2,*} , Manuel Ventura ¹ and C. Guedes Soares ¹ 

¹ Centre for Marine Technology and Ocean Engineering (CENTEC), Instituto Superior Técnico, Universidade de Lisboa, Av. Rovisco Pais 1, 1049-001 Lisboa, Portugal; manuel.ventura@centec.tecnico.ulisboa.pt (M.V.); c.guedes.soares@centec.tecnico.ulisboa.pt (C.G.S.)

² Department of Naval Architecture and Marine Engineering, Faculty of Engineering, Alexandria University, Alexandria 21544, Egypt

* Correspondence: mina.tadros@centec.tecnico.ulisboa.pt

Abstract: The effects of hull and propeller roughness are presented over ten years of operation on ship performance. The developed model used in this study is a combination of NavCad and Matlab to perform the resistance and propulsion computations of the selected ship as well as the processing of input and output data. By considering the ship hull, the engine installed and an optimized propeller, the ship performance is computed for a different combination of hull and propeller roughness according to the ITTC recommendations and the opinion of experts in the marine field. Twelve cases are simulated over the selected years of operations and compared to the new ship performance. The hull roughness has the dominant effect on the performance of the ship due to its large area. However, by adding the effect of propeller roughness, an increment is noticed in the loading ratio and fuel consumption by 1–4% and 2–4%, respectively, in addition to the hull roughness. From this study, it is concluded that the roughness of both the hull and propeller is important consider to achieve more accurate results than just considering the hull roughness.

Keywords: bulk carrier; propeller roughness; fuel consumption; energy efficiency; cavitation



Citation: Tadros, M.; Ventura, M.; Guedes Soares, C. Effect of Hull and Propeller Roughness during the Assessment of Ship Fuel Consumption. *J. Mar. Sci. Eng.* **2023**, *11*, 784. <https://doi.org/10.3390/jmse11040784>

Academic Editor: Sergejus Lebedevas

Received: 16 March 2023

Revised: 2 April 2023

Accepted: 3 April 2023

Published: 5 April 2023



Copyright: © 2023 by the authors. Licensee MDPI, Basel, Switzerland. This article is an open access article distributed under the terms and conditions of the Creative Commons Attribution (CC BY) license (<https://creativecommons.org/licenses/by/4.0/>).

1. Introduction

A great effort is made by the International Maritime Organization (IMO) and the recognized organizations to improve the energy efficiency of the maritime fleet by reducing the amount of exhaust emissions, mainly carbon dioxide (CO₂), compared to the ship transport work [1,2]. The different stakeholders have proposed several technologies and solutions to ensure the transition in the maritime industry towards the concept of sustainability [3–5]. These solutions can be applied in the short term, such as the application of energy efficiency measures and performing some retrofit solutions to reduce the level of consumption and emissions [6–8] or in the long term by using several alternative fuels to significantly cut the level of emissions from the prime mover of the ships, in particular, the total annual greenhouse gas (GHG), by at least 50% by 2050 [9–11].

The main objective of the regulations is to reduce the CO₂ emissions from ship engines as they depend on fuel consumption. Therefore, it is essential to consider a smooth and clean hull to achieve the minimum amount of ship resistance and, thus, reduce the power required and to select a suitable propeller to move the ships as well as the fuel consumption [12,13]. The generation process of the hull lines corresponding to the ship dimension becomes the important step in reducing the ship resistance during the stages of ship design [14–16] as well as in operation when encountering waves [17–22].

In addition to the hull form, ship roughness is an important factor that affects the energy efficiency of the ship. It refers to the irregularities on the surface of the hull, thus increasing the total resistance, resulting in a loss in the ship speed, higher fuel consumption

and operating costs. Various factors, including marine growth, paint fouling and corrosion, can cause the roughness of a ship, as described by Daidola [23].

The reduction of ship roughness can improve the energy efficiency of the ship. One common method is applying specialized coatings to the hull, such as low-friction, antifouling and self-polishing coatings. These coatings can help reduce the build-up of marine growth and other debris on the hull, reducing the roughness and improving the hydrodynamic performance of the ship. Recently, the transition toward using biomass coating, such as Tannin-FeIII (TA-FeIII) has become a solution and alternative to typical phlorotannin, which is eco-friendly, safe and cost effective [24]. DNV [25] provided complete guidelines for ship protection from corrosion and the type of painting material used for each hull. Further, regular hull cleaning and maintenance are required to reduce surface roughness over the years of operation. According to the International Convention for the Safety of Life at Sea (SOLAS) [26], at least two inspections of the outside of the ship's bottom shall be carried out during any five years to ensure the safety of the hull and the smooth operation of the vessel.

These types of inspections can avoid the increase of the level of the average hull roughness (AHR) by more than 10 μm per year [27], which significantly increases the ship resistance and, thus, the fuel consumption, which can reach 12 tons/day in the case of a ship tanker, as reported by Smith and Colvin [28].

Most of the studies focused on assessing ship performance at a different level of hull roughness because it is the greatest contributor to ship resistance. Song et al. [29] used computational fluid dynamics (CFD) to predict the total ship resistance with the occurrence of roughness and validate the model using experimental results. The model shows a good agreement with real data, where the friction and viscous resistance increase while the wave-making resistance decreases. Sun et al. [30] used the CFD model to estimate the ship performance, showing good agreement with the experimental results as well. They concluded that the value of roughness must be considered during the simulation as an important factor which increases the delivered power by 7%. Farkas et al. [31] demonstrated a reduction in ship speed by 2 knots as the delivered power increased by 36.3%, and the impact of the biofouling could change according to the ship hull form [32]. By comparing several hull forms, as in [33], the rough hull with a bulbous bow shows a higher added resistance than the normal hull. Mikkelsen and Walther [34] showed that the accuracy of the delivered power of the ship from CFD is within 8–12% compared to the experimental data, which is considered an acceptable range compared to similar research comparing CFD with empirical formulas or experimental tests [35,36]. The same conclusion has been supported by García et al. [37], showing that the CFD models are easily able to estimate the ship performance with the existence of roughness.

However, considering the roughness of the propeller during the simulation is important to achieve high accuracy. Due to the complicated simulation process, especially when it is rotating, few papers have considered the effect of propeller roughness on its performance and the overall ship performance. Song et al. [38] used CFD to evaluate the performance of the propeller in open water conditions. They concluded a reduction in open propeller efficiency as the propeller thrust coefficient decreases while the propeller torque coefficient increases. Asnaghi et al. [39] concluded that the balance between the mitigation of tip vortex cavitation and performance degradation could be achieved by having roughness on the blade tip as well as a limited area on the leading edge; otherwise, the overall performance will be worse. While the roughness has some negative effects, Sezen et al. [40] noticed some positive effects from the existence of roughness as it reduces the cavitation volume and noise level. According to Carchen and Atlar [41], the common parameters of the propeller are not sufficient to evaluate the effect of fouling on ship performance. Therefore, more key performance indicators (KPIs) are defined, including wake fraction gain, apparent wake fraction gain and the fouling coefficient, to give more insight into the effect of fouling on the ship performance losses compared to the given baseline.

While the existing detailed model is essential to understand the behaviour of the system behaviour in 3D models, using the empirical formulas in a holistic model has advantages in computing the overall ship performance with high accuracy in a reasonable time. Therefore, this paper contributes to the prediction of the performance of a given ship and the attached propeller in terms of hydrodynamics and its effect on the computation of fuel consumption from the concept of design and operation in calm water at different combined hull and propeller roughness levels to assess the overall ship performance over the years.

The remainder of this paper is organized as follows. First, the numerical model used to perform the simulation is presented in detail in Section 2. Next, the computed results and the evaluation of the ship, engine and propeller performance in both calm water and different weather conditions are presented in Section 3. Finally, a summary of the main findings and recommendations for future work are presented in Section 4.

2. Numerical Model

The main structure of the numerical model used in this study is a combination between NavCad [42] and Matlab through an application programming interface (API), previously developed in [43]. This model is used to simulate different types of studies based on optimization procedures, such as maximizing propeller efficiency and minimizing fuel consumption, comparing the performance of different types of propellers.

The model is developed in a Matlab environment to easily process the input and output data according to the requirement of the objective and constraints of the optimization problem as well as the required results. For instance, the model is able to select a controllable pitch propeller (CPP) [44] or contra-rotating propeller (CRP) [45] at the engine operating point with minimum fuel consumption as a way to find solutions towards the reduction of fuel consumption.

The model has been then extended to consider the effect of hull roughness on the ship resistance, and thus the power and the amount of fuel consumption over ten years of operation [46]. Based on the last study, the effect of propeller roughness is added to the model to study the overall performance of the ship when subjected to hull and propeller roughness. This paper uses the same bulk carrier ship to perform the numerical simulation. The ship has a 154 m length, with a propulsion system composed of a four-stroke marine diesel engine, a reduction gearbox, a transmission shaft and a single fixed-pitch propeller (FPP). The main characteristics of the ship, engine and optimized propeller are given in Table 1.

Regarding the ship, the main parameters of the ship have been collected from the hull form of the ship at the design conditions and defined in the suitable section in NavCad in order to compute the ship resistance. Then, the total calm water resistance is calculated using the methods presented at the International Towing Tank Conference (ITTC-78) [47], as in the following expression:

$$C_T = (1 + k)C_F + C_R + C_A + \Delta C_F \quad (1)$$

where C_T is the total resistance coefficient, C_F is the frictional resistance coefficient, k is the hull form factor as mentioned in the ITTC-57 [48], C_R is the residuary resistance coefficient, C_A is the correlation allowance and ΔC_F is the roughness allowance computed using the following equation:

$$\Delta C_F = 0.044 \left[\left(\frac{k_s}{L_{WL}} \right)^{\frac{1}{3}} - 10Re^{-\frac{1}{3}} \right] + 0.000125 \quad (2)$$

where k_s is the roughness of the hull surface as defined by the designer, L_{WL} is the ship length at the water line and Re is the Reynolds number.

Table 1. Main characteristics of the bulk carrier [46].

	Characteristics	Symbol	Unit	Value
Ship characteristics	Length at waterline	L_{WL}	m	154.00
	Breadth	B	m	23.11
	Draft	T	m	10.00
	Displacement	Δ	tonne	27,690
	Service speed	V_0	knot	14.5
	Maximum speed	V_{max}	knot	16.0
	Number of propellers	N_p	-	1
	Type of propellers	-	-	FPP
	Rated power	P_{max}	kW	7140
Engine characteristics	Engine builder	-	-	MAN Energy Solutions [49]
	Brand name	-	-	MAN
	Bore	B	mm	320
	Stroke	S	mm	440
	Displacement	V	litre	4954
	Number of cylinders	n_c	-	14
	Rated speed	RPM_{max}	rpm	750
	Rated power	P_{max}	kW	7140
Propeller characteristics	Speed at 14.5 knot	RPM	rpm	714
	Series	-	-	Wageningen B-series
	Diameter	D	m	6.0
	Expanded area ratio	EAR	-	0.47
	Pitch diameter ratio	P/D	-	1.097
	Gearbox ratio	GBR	-	9.5
Propeller characteristics	Number of blades	Z	-	5
	Speed at 14.5 knot	N	rpm	75

Regarding the engine, its performance has been optimized using a developed optimization model presented in [50] taking into account all of the thermodynamic properties along the engine parts [51,52]. The optimization procedures are performed along the engine load diagram, where the results are presented by a polynomial equation as a surrogate model to easily be used in other studies [53,54], allowing more flexibility to be integrated into other numerical models [55]. Due to the similar behaviour of the engines in the same series, the original engine is modelled with a 9180 kW rated power and then scaled to 7140 kW to fit the selected ship.

Regarding the propeller, the propeller geometry and the operational point are selected at a clean hull using an optimization model developed in [56]. The gearbox ratio (GBR) is selected as the ratio between the engine and propeller speed, and the gearbox and transmission shaft efficiencies are kept constant (97%).

By defining the propeller series and the number of blades, the propeller is designed after computing the total resistance of the ship hull using the methods presented in [57,58] and then the wake fraction (w) and thrust deduction fraction (t) as propulsive coefficients are computed using the methods presented in [59]. This method shows effectiveness during the computation compared with the results from CFD models [35].

The advance coefficient (J_A), thrust coefficient (K_T), torque coefficient (K_Q) and the propeller efficiency (η_o) are computed to evaluate the propeller performance, as presented in the following expressions [60]:

$$J_A = \frac{V_A}{nD} \tag{3}$$

$$K_T = \frac{T}{\rho_w n^2 D^4} \tag{4}$$

$$K_Q = \frac{Q}{\rho_w n^2 D^5} \tag{5}$$

$$\eta_o = \frac{K_T J_A}{K_Q 2\pi} \tag{6}$$

where V_A is the advance speed, n is the propeller speed, ρ_w is the water density, T is the propeller thrust and Q is the propeller torque.

However, according to the ITTC-78, the roughness of the propeller is taken into account by considering the increased changes in drag (D) and the decreased changes in the lift (L) when computing the thrust and torque coefficients as in the following equations:

$$K_{TR} = K_{TS} - \Delta K_{TD} - \Delta K_{TL} \tag{7}$$

$$K_{QR} = K_{QS} - \Delta K_{QD} - \Delta K_{QL} \tag{8}$$

where,

$$\Delta K_{TD} = -\Delta C_D \times 0.3 \times \frac{P}{D} \frac{cZ}{D} \tag{9}$$

$$\Delta K_{QD} = \Delta C_D \times 0.25 \times \frac{cZ}{D} \tag{10}$$

$$\Delta K_{TL} = \Delta C_L \times \frac{cZ}{D} \frac{0.733 + 0.132J^2}{\sqrt{1 + 0.18(\frac{P}{D})^2}} \tag{11}$$

$$\Delta K_{QL} = \Delta C_L \times \frac{cZ}{D} \frac{0.117 + 0.021J^2}{\sqrt{1 + 0.18(\frac{P}{D})^2}} \tag{12}$$

where K_{TR} and K_{QR} are thrust and torque coefficients for the rough propeller, while K_{TS} and K_{QS} are thrust and torque coefficients for the smooth propeller. ΔK_{TD} and ΔK_{TL} are the changes in thrust coefficient due to drag and lift, while ΔK_{QD} and ΔK_{QL} are the changes in torque coefficient due to drag and lift. C_D is the drag coefficient, C_L is the lift coefficient, P is the propeller pitch, D is the propeller diameter, Z is the number of blades, c is the chord length at $0.75 R$ and R is the propeller radius.

Different criteria are considered during the simulation as constraints. They include cavitation and noise parameters to ensure the safety and durability of the propulsion system, as described in detail in [61].

To better evaluate the system performance for different roughness levels, the fuel consumption is computed in kg/nm taking into account the brake-specific fuel consumption (BSFC), brake power (P_B) and ship service speed using the following expression:

$$FC_{kg/nm} = \frac{BSFC \times P_B \times 1000}{V_S} \tag{13}$$

After optimizing the propeller in calm water by taking the standard values of roughness for both hull (15 mm) and propeller (0.03 mm), these values have been changed according to the recommendations of ITTC [47] and of the experts in [23,62], where the propeller roughness is computed for each year. The schematic diagram of the simulation process is presented in Figure 1.

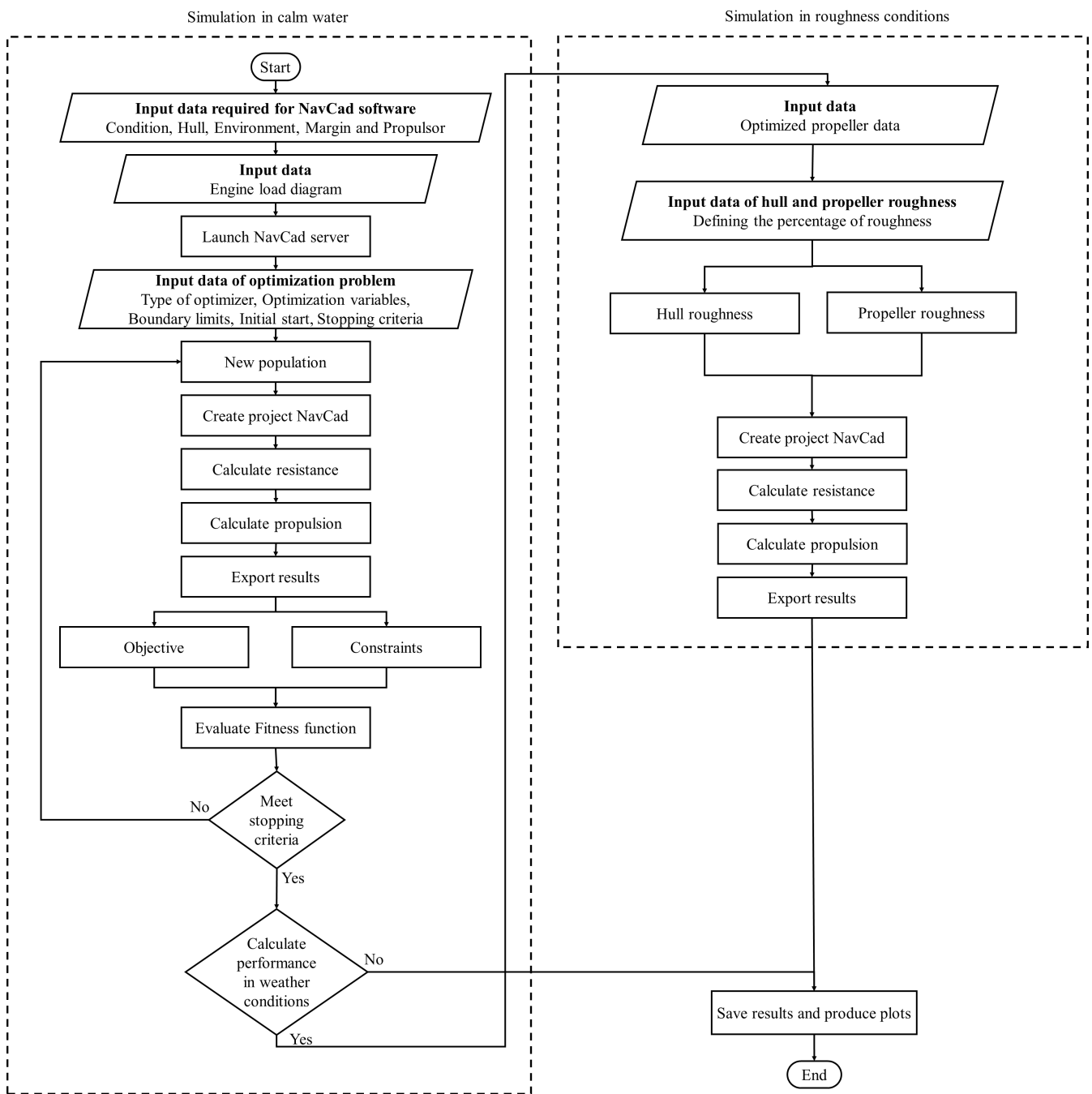


Figure 1. Schematic diagram of the simulation process.

3. Results

According to the previous computation performed in [61], the propeller geometry and the gearbox ratio have been optimized during the design stage of the ship at zero roughness, as described in Figure 1. This type of calculation is performed at the final stage of the overall computation after computing the ship resistance based on the hull dimensions collected from the 3D hull, followed by the estimation of the power required to force the ship at a given speed. While the propeller selection is performed on new ships to give the required thrust and ensure the safety of the propulsion system and the surrounding environment, some changes can be noticed over the years due to the existing roughness of the hull and propeller to evaluate the energy efficiency of the ship over the years.

This paper considers the effect of roughness by presenting twelve cases of computation of different hull and propeller roughness combinations over ten years of operations. The

values of roughness have been considered based on the recommendations of the ITTC [63] and previously papers published [62] due to the fouling of the hull and the attached propeller over the years. Table 2 presents the different configurations of the ship conditions, including the level of roughness for the hull and propeller, where the performance of the ship is affected over the years of operation.

Table 2. Configurations of the simulated cases for different hull and propeller roughness.

Cases	Age of Ship (Years)	Condition of Ship	Hull Roughness (mm)	Propeller Roughness (mm)
1	zero	New ship	0.15	0.0
2	zero	New ship	0.15	0.03
3	two	Rough ship	0.35	0.0
4	two	Rough ship	0.35	0.09
5	five	Clean ship	0.4	0.0
6	five	Clean ship	0.4	0.12
7	five	Rough ship	0.5	0.0
8	five	Rough ship	0.5	0.15
9	ten	Clean ship	0.55	0.0
10	ten	Clean ship	0.55	0.04
11	ten	Rough ship	0.65	0.0
12	ten	Rough ship	0.65	0.23

The calculated results are presented in Table A1 in Appendix A for more information, and the changes in propeller and engine performance are presented in Figures 2–4. The first simulated case (New ship) is considered as the reference case study, and the percentage of change of the different parameters according to the level of roughness is computed and compared to it. The results show that the hull roughness has the dominant effect on the ship performance; however, the propeller roughness shall be considered to achieve highly accurate results.

Regarding the propeller characteristics, as presented in Figure 2, five main parameters of the propeller behind the hull are presented, showing changes over the years when applying the effect of hull and propeller roughness.

The propeller speed is increased over the years by up to 4%. The effect of propeller roughness is not noticed when it is considered among all simulated cases, except in the case of the rough ship after two years of operation, where the propeller speed is increased by 1.5%.

The same behaviour is followed by the propeller thrust, where the required thrust is increased by around 10% after ten years of operations, depending on the roughness level. The propeller roughness does not show any effect when it is considered during the simulation.

Regarding the propeller torque, an increment in the computed values is noticed and increased by up to 12% over the years. The propeller roughness has an effect on the propeller torque and can increase its values by 0.3–3% according to the years of operation compared to the same case that considered the hull roughness only. For instance, by considering 0.09 mm propeller roughness, the propeller torque can increase by 1.5% compared to the same case with 0.0 mm propeller roughness, while this value can reach 3% when the propeller roughness is 0.23 mm compared to the same case with hull roughness only. This change is directly affected by the amount of drag and lift as computed from the equations in the previous section.

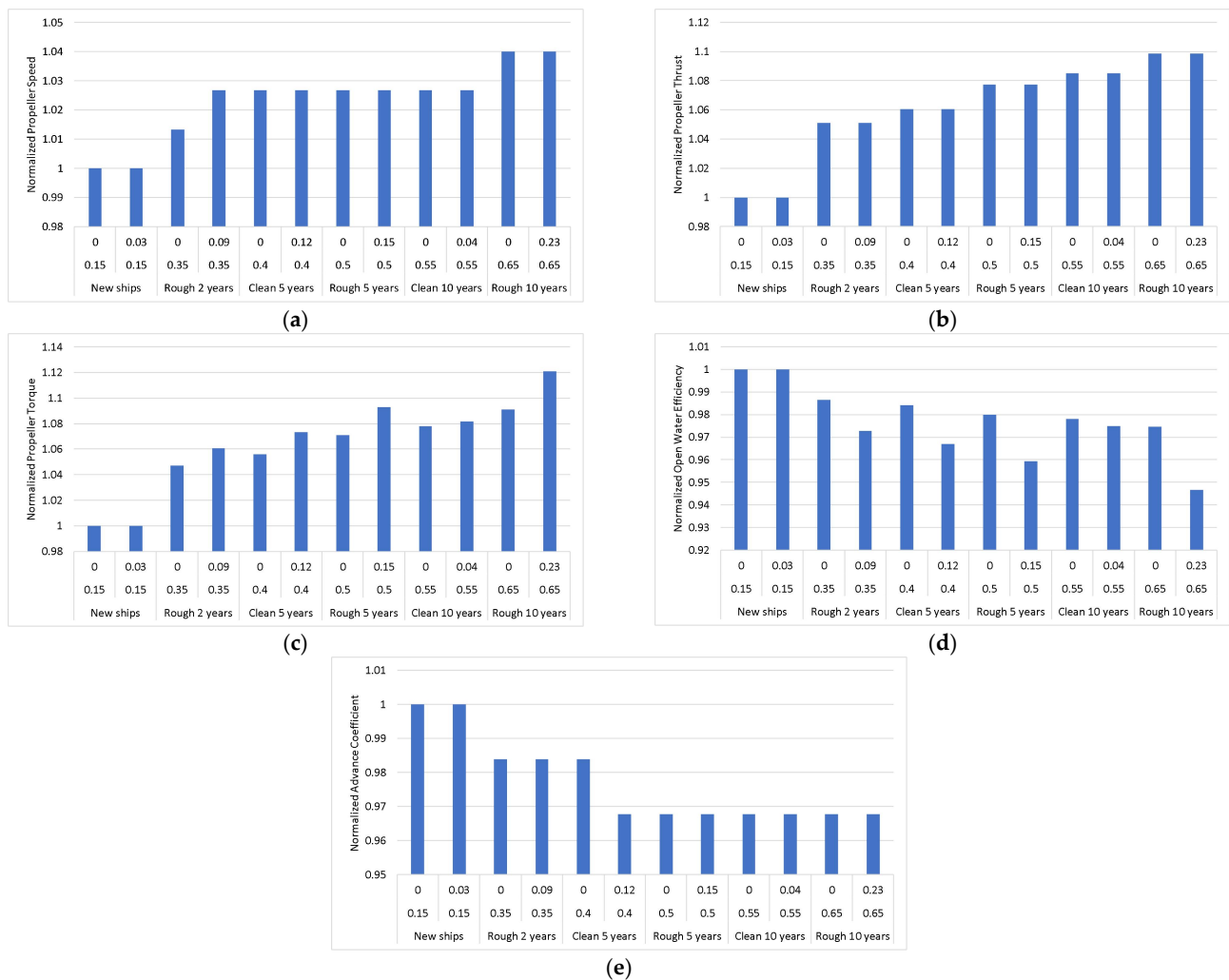


Figure 2. Propeller characteristics at different hull and propeller roughness: (a) propeller speed, (b) propeller thrust, (c) propeller torque, (d) open water efficiency and (e) advance coefficient.

As the open water efficiency is directly computed as a function of thrust and torque, a decrease in its values with the same amount of increasing torque is noticed over the years, showing the maximum amount of reduction after ten years of operation.

A slight reduction in the advance coefficient is noticed due to the variation of propeller speed, as described before, which is the main parameter that shows a deviation among the simulated cases.

From Table A1, the thrust and torque coefficients as well as the wake fraction and thrust deduction factor of all simulated cases show a very slight reduction, which is not noticed when the values are approximated to two decimal points. This is because these values are assumed constant over ten years of ship operation, following the same concept presented in detail in [64].

Regarding the cavitation and noise criteria, five main parameters are considered and presented in Figure 3 to evaluate the system’s durability and safety.

The tip speed, in general, increases by up to 3.5% after ten years of operation; however, a slight increment is noticed when considering the propeller roughness in the simulation. This increment can reach 0.2% for old ships than new ships.

Regarding the minimum EAR, average loading pressure and back cavitation, there is a general increment in the behaviour of each parameter over the years, reaching around 6%, 10% and 19%, respectively, compared to the reference case. However, the propeller roughness did not show a noticeable effect when it was considered in the simulation.

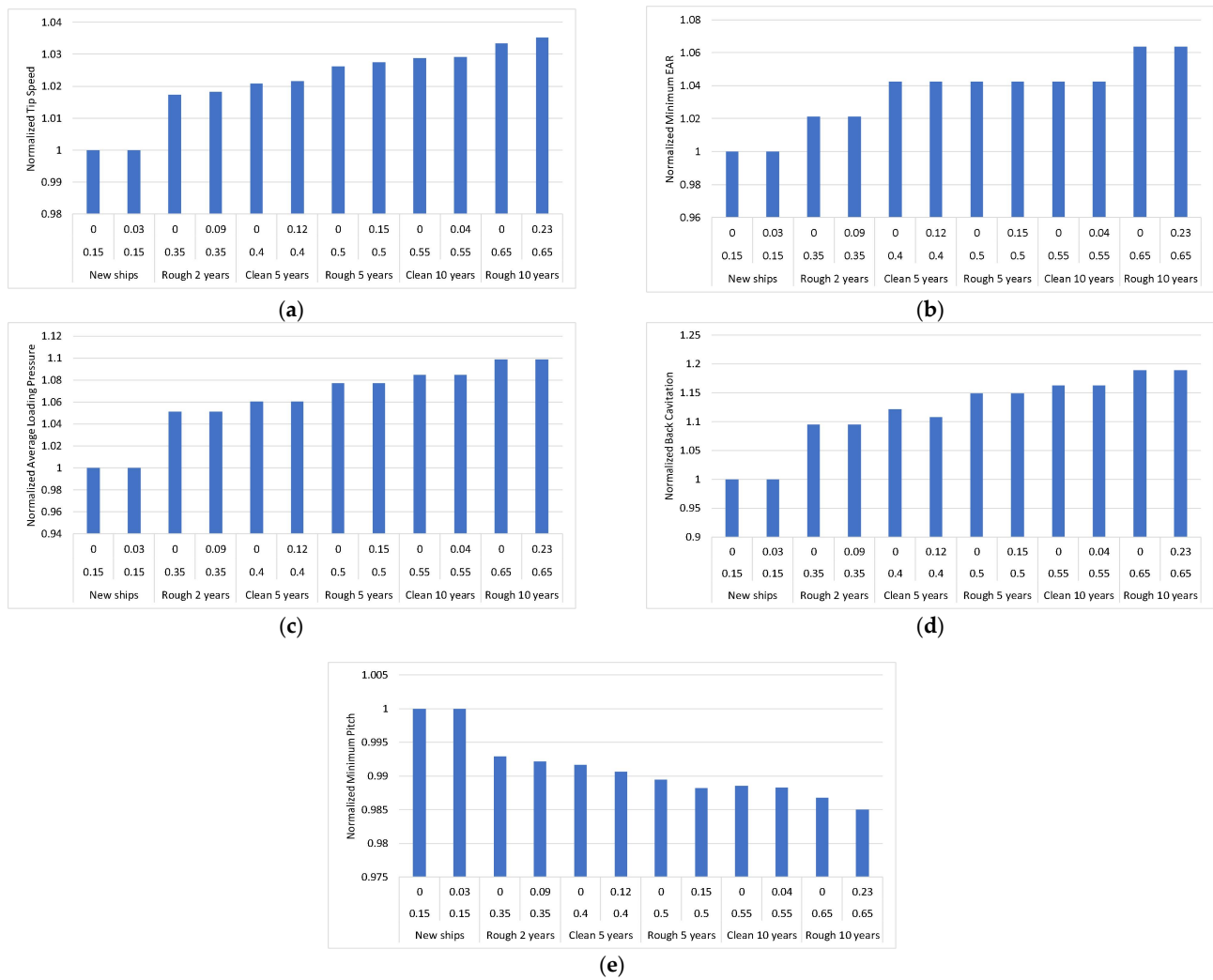


Figure 3. Cavitation criteria at different hull and propeller roughness; (a) tip speed, (b) minimum EAR, (c) average loading pressure, (d) back cavitation and (e) minimum pitch.

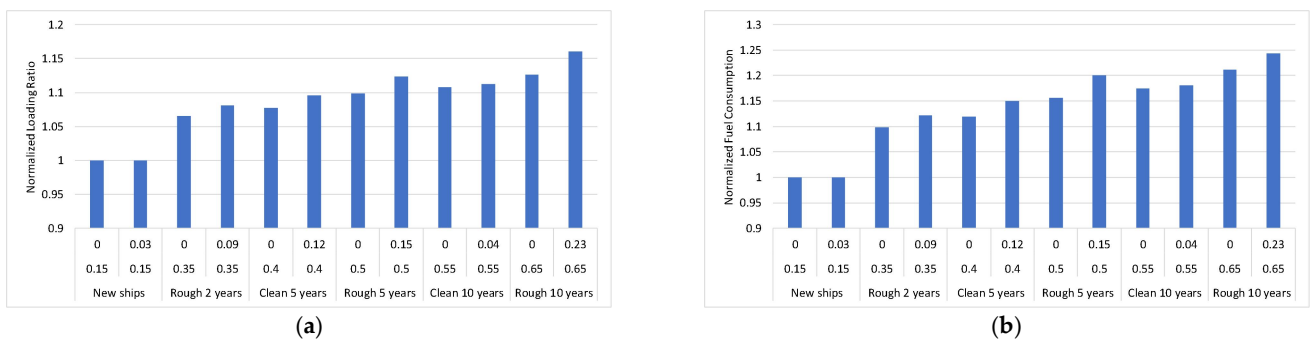


Figure 4. Engine characteristics at different hull and propeller roughness; (a) loading ratio and (b) fuel consumption.

In the computation of the last parameter to avoid face cavitation, the values of the minimum pitch are reduced along the years by around 1.5%; however, the propeller roughness has a very small effect of less than 0.25% among the cases. This parameter is directly affected by the changes that occurred in both the advance coefficient and thrust coefficient, as described in [65].

Regarding engine performance, the loading ratio and fuel consumption are computed to evaluate the overall system, as shown in Figure 4.

There is a big change in the loading ratio over the years when considering the effect of hull roughness compared to the reference case. This value can increase the loading ratio by 12.5%, while this value can have a greater increase with the consideration of the propeller roughness, reaching around 16% compared to new ships. This difference can vary according to the roughness level showing an increase of 1 to 4% compared to the performance of the new ship, based on the year of operation and the cleanness of the hull and propeller.

As the loading ratio increases, the fuel consumption also increases. Considering the hull and propeller roughness, the fuel consumption can increase by up to 24% after ten years compared to 21% only in the case of hull roughness only; these two values are compared to the case of new ships. When considering the propeller roughness, this difference can vary between 2 and 4% as a reference to new ships and compared to computation performed in the case of hull roughness only.

4. Conclusions

This paper presents the effect of hull and propeller roughness over ten years of operation on the ship's performance in calm water. The performance of the ship is computed based on a given hull and engine of a bulk carrier, where the propeller is selected and optimized at the engine operating point with minimum fuel consumption. Twelve cases are considered combining different levels of the hull and propeller roughness over the selected period of ship operation. The roughness levels are defined based on the ITTC recommendations and the opinion of experts in the field. This kind of study helps to provide more accurate results of the ship performance after several years of operation compared to a new one.

It has been concluded from this study that:

1. The developed numerical model can easily estimate the performance of the ship at different roughness levels.
2. The roughness of the hull has had a dominant effect on the ship performance over the years.
3. The consideration of propeller roughness can provide more accurate results than just considering the hull roughness alone.
4. While there is an increment in the loading ratio of the engine due to hull roughness over the years, reaching up to 12.5% more compared to a new ships, the consideration of propeller roughness can increase this value by 1 to 4 % of the loading ratio of new ships according to the level of cleanness of the hull and propeller.
5. Based on the previous point, the fuel consumption is also increased by 2 to 4% when considering the propeller roughness besides the percentage increase due to hull roughness.
6. Finally, it is recommended to consider the effect of the roughness of both hull and propeller in order to ensure highly accurate results, rather than considering only the effect of hull roughness.

Due to the development of the installation of sensors onboard, further works will be planned to measure and evaluate the ship performance over the years with several roughness conditions to provide correction factors for each ship type. This will help to provide a machine learning model to be installed onboard to assist the ship master in taking the right decision [66].

Author Contributions: The concept of the problem is developed by M.T. The analysis is performed by M.T. and the writing of the original draft manuscript is done by M.T., M.V. and C.G.S. All authors have read and agreed to the published version of the manuscript.

Funding: This work was performed within the scope of the Strategic Research Plan of the Centre for Marine Technology and Ocean Engineering (CENTEC), which is financed by the Portuguese

Foundation for Science and Technology (Fundação para a Ciência e Tecnologia-FCT) under contract UIDB/UIDP/00134/2020.

Institutional Review Board Statement: Not applicable.

Informed Consent Statement: Not applicable.

Data Availability Statement: The data presented in this study are available on request from the corresponding author.

Conflicts of Interest: The authors declare no conflict of interest.

Abbreviations

3D	Three dimensional
AHR	Average hull roughness
B	Breadth
B	Bore
BSFC	Brake-specific fuel consumption
c	Chord length at radius 0.75 R
C_A	Correlation allowance
C_D	Drag coefficient
C_F	Frictional coefficient
CFD	Computational fluid dynamics
C_L	Lift coefficient
CO ₂	Carbon dioxide
CPP	Controllable pitch propeller
C_R	Residuary resistance coefficient
CRP	Contra-rotating propeller
C_T	Total resistance coefficient
D	Propeller diameter
D	Drag
EAR	Expanded area ratio
FPP	Fixed-pitch propeller
GBR	Gearbox ratio
GHG	Greenhouse gas
IMO	International Maritime Organization
ITTC	International Towing Tank Conference
J_A	Advance coefficient
k	Hull form factor
KPI	Key performance indicators
K_Q	Torque coefficient
K_{QR}	Torque coefficient for the rough propeller
K_{QS}	Torque coefficient for the smooth propeller
k_s	Roughness of the hull surface
K_T	Thrust coefficient
K_{TR}	Thrust coefficient for the rough propeller
K_{TS}	Thrust coefficient for the smooth propeller
L	Lift
L_{WL}	Ship length at waterline
n	Propeller speed
N	Propeller speed in rpm
n_c	Number of cylinders
N_P	Number of propellers
P/D	Pitch diameter ratio
P_B	Brake power
P_{max}	Rated power
Q	Propeller torque

R	Propeller radius
Re	Reynolds number
RPM_{max}	Rated speed
S	Stroke
SOLAS	International Convention for the Safety of Life at Sea
t	Thrust deduction factor
T	Propeller thrust
T	Draft
V	Engine displacement
V_A	Advance speed
V_s	Ship design speed
V_{s-max}	Ship maximum speed
w	Wake fraction
Z	Number of propeller blades
Δ	Ship displacement
ΔC_F	Roughness allowance
ΔK_{QD}	Changes in torque coefficient due to drag
ΔK_{QL}	Changes in torque coefficient due to lift
ΔK_{TD}	Changes in thrust coefficient due to drag
ΔK_{TL}	Changes in thrust coefficient due to lift
η_o	Open-water propeller efficiency
ρ_w	Water density

Appendix A

Table A1. Optimum results for different configurations.

Main Characteristics	Parameters	Unit													
Level of Roughness	Ship age	[years]	New ships		Rough 2 years		Clean 5 years		Rough 5 years		Clean 10 years		Rough 10 years		
	Hull Roughness	[mm]	0.15	0.15	0.35	0.35	0.40	0.40	0.50	0.50	0.55	0.55	0.65	0.65	
	Propeller Roughness	[mm]	0.00	0.03	0.00	0.09	0.00	0.12	0.00	0.15	0.00	0.04	0.00	0.23	
Ship characteristics	Ship speed	[kn]	14.50	14.50	14.50	14.50	14.5	14.50	14.50	14.50	14.5	14.50	14.5	14.50	
Propeller characteristics	Series	[-]	Wageningen B-series												
	Cup	[%]	0.00	0.00	0.00	0.00	0.00	0.00	0.00	0.00	0.00	0.00	0.00	0.00	
	Diameter	[m]	6.00	6.00	6.00	6.00	6.00	6.00	6.00	6.00	6.00	6.00	6.00	6.00	
	Expanded area ratio	[-]	0.47	0.47	0.47	0.47	0.47	0.47	0.47	0.47	0.47	0.47	0.47	0.47	
	Pitch	[m]	6.58	6.58	6.58	6.58	6.58	6.58	6.58	6.58	6.58	6.58	6.58	6.58	
	Speed	[rpm]	75.00	75.00	76.00	77.00	77.00	77.00	77.00	77.00	77.00	77.00	77.00	78.00	78.00
	Thrust	[kN]	576.50	576.50	605.99	605.99	611.45	611.45	621.13	621.13	625.49	625.49	633.47	633.47	
	Torque	[kN.m]	573.30	573.30	600.30	608.20	605.3	615.40	614.10	626.60	618.1	620.00	625.4	642.70	
	Open water efficiency	[%]	59.32	59.32	58.52	57.71	58.38	57.36	58.13	56.90	58.02	57.83	57.81	56.16	
	Advance coefficient	[-]	0.62	0.62	0.61	0.61	0.61	0.60	0.60	0.60	0.60	0.60	0.60	0.60	
	Thrust coefficient	[-]	0.28	0.28	0.28	0.28	0.28	0.28	0.28	0.28	0.28	0.28	0.28	0.28	
	Torque coefficient	[-]	0.05	0.05	0.05	0.05	0.05	0.05	0.05	0.05	0.05	0.05	0.05	0.05	
Wake fraction	[-]	0.38	0.38	0.38	0.38	0.38	0.38	0.38	0.38	0.38	0.38	0.38	0.38		
Thrust deduction factor	[-]	0.19	0.19	0.19	0.19	0.19	0.19	0.19	0.19	0.19	0.19	0.19	0.19		
Cavitation and noise criteria	Tip Speed	[m/s]	23.61	23.61	24.02	24.04	24.10	24.12	24.23	24.26	24.29	24.30	24.40	24.44	
	Minimum expanded area ratio	[-]	0.47	0.47	0.48	0.48	0.49	0.49	0.49	0.49	0.49	0.49	0.50	0.50	
	Average loading pressure	[kPa]	43.57	43.57	45.80	45.80	46.21	46.21	46.94	46.94	47.27	47.27	47.87	47.87	
	Back Cavitation	[%]	7.40	7.40	8.10	8.10	8.30	8.20	8.50	8.50	8.60	8.60	8.80	8.80	
	Minimum pitch	[m]	4978.5	4978.5	4943.4	4939.3	4937.1	4931.9	4926.2	4919.8	4921.3	4920.3	4912.5	4903.8	
Gearbox characteristics	Gearbox ratio	[-]	9.5	9.5	9.5	9.5	9.5	9.5	9.5	9.5	9.5	9.5	9.5	9.5	
Engine characteristics	Speed	[rpm]	714	714	727	727	729	730	733	734	735	735	738	740	
	Brake Power	[kW]	4682.3	4682.3	4988.6	5058.8	5045.9	5135.9	5147.9	5259.1	5194.1	5211.0	5278.9	5434.8	
	Loading ratio	[%]	65.60	65.60	69.90	70.90	70.7	71.90	72.10	73.70	72.7	73.00	73.9	76.10	
	BSFC	[g/kW.h]	191.8	191.8	197.8	199.1	199.1	201.2	201.8	204.9	203.1	203.6	206.1	205.5	
	Fuel consumption	[kg/nm]	61.93	61.93	68.04	69.47	69.29	71.25	71.64	74.34	72.77	73.16	75.02	77.03	

References

1. IMO. Energy Efficiency Measures. IMO. Available online: <http://www.imo.org/en/ourwork/environment/pollutionprevention/airpollution/pages/technical-and-operational-measures.aspx> (accessed on 5 June 2016).
2. Karatuğ, Ç.; Arslanoğlu, Y.; Guedes Soares, C. Evaluation of decarbonization strategies for existing ships. In *Trends in Maritime Technology and Engineering*; Guedes Soares, C., Santos, T.A., Eds.; Taylor & Francis Group: London, UK, 2022; pp. 45–54.
3. Mallouppas, G.; Yfantis, E.A. Decarbonization in Shipping Industry: A Review of Research, Technology Development, and Innovation Proposals. *J. Mar. Sci. Eng.* **2021**, *9*, 415. [[CrossRef](#)]
4. Stark, C.; Xu, Y.; Zhang, M.; Yuan, Z.; Tao, L.; Shi, W. Study on Applicability of Energy-Saving Devices to Hydrogen Fuel Cell-Powered Ships. *J. Mar. Sci. Eng.* **2022**, *10*, 388. [[CrossRef](#)]
5. Butterworth, J.; Atlar, M.; Shi, W. Experimental analysis of an air cavity concept applied on a ship hull to improve the hull resistance. *Ocean Eng.* **2015**, *110*, 2–10. [[CrossRef](#)]
6. Green Ship of the Future. 2019 Retrofit Project. Available online: <https://greenship.org/project/2019-retrofit-series/> (accessed on 8 December 2021).
7. Karatuğ, Ç.; Arslanoğlu, Y.; Guedes Soares, C. Feasibility Analysis of the Effects of Scrubber Installation on Ships. *J. Mar. Sci. Eng.* **2022**, *10*, 1838. [[CrossRef](#)]
8. Stark, C.; Shi, W.; Atlar, M. A numerical investigation into the influence of bio-inspired leading-edge tubercles on the hydrodynamic performance of a benchmark ducted propeller. *Ocean Eng.* **2021**, *237*, 109593. [[CrossRef](#)]
9. DNV. *Maritime Forecast to 2050: Energy Transition Outlook 2020*; DNV: Bærum, Norway, 2020.
10. Stoumpos, S.; Theotokatos, G. Multiobjective Optimisation of a Marine Dual Fuel Engine Equipped with Exhaust Gas Recirculation and Air Bypass Systems. *Energies* **2020**, *13*, 5021. [[CrossRef](#)]
11. Elkafas, A.G.; Elgohary, M.M.; Shouman, M.R. Numerical analysis of economic and environmental benefits of marine fuel conversion from diesel oil to natural gas for container ships. *Environ. Sci. Pollut. Res.* **2021**, *28*, 15210–15222. [[CrossRef](#)]
12. Ventura, M. Ship dimensioning in the initial design. In *Developments in Maritime Transportation and Exploitation of Sea Resources*; Guedes Soares, C., López Peña, F., Eds.; Taylor & Francis Group: London, UK, 2014; pp. 531–539.
13. Tadros, M.; Ventura, M.; Guedes Soares, C. An optimisation procedure for propeller selection for different shaft inclinations. *Int. J. Marit. Eng.* **2022**, *164*, 295–315. [[CrossRef](#)]
14. Liu, X.; Zhao, W.; Wan, D. Hull form optimization based on calm-water wave drag with or without generating bulbous bow. *Appl. Ocean Res.* **2021**, *116*, 102861. [[CrossRef](#)]
15. Zha, L.; Zhu, R.; Hong, L.; Huang, S. Hull form optimization for reduced calm-water resistance and improved vertical motion performance in irregular head waves. *Ocean Eng.* **2021**, *233*, 109208. [[CrossRef](#)]
16. Wang, S.M.; Duan, F.; Li, Y.; Xia, Y.K.; Li, Z.S. An improved radial basis function for marine vehicle hull form representation and optimization. *Ocean Eng.* **2022**, *260*, 112000. [[CrossRef](#)]
17. Duan, W.; Li, C. Estimation of added resistance for large blunt ship in waves. *J. Mar. Sci. Appl.* **2013**, *12*, 1–12. [[CrossRef](#)]
18. Liu, S.; Shang, B.; Papanikolaou, A.; Bolbot, V. Improved formula for estimating added resistance of ships in engineering applications. *J. Mar. Sci. Appl.* **2016**, *15*, 442–451. [[CrossRef](#)]
19. Park, D.-M.; Lee, J.-H.; Jung, Y.-W.; Lee, J.; Kim, Y.; Gerhardt, F. Experimental and numerical studies on added resistance of ship in oblique sea conditions. *Ocean Eng.* **2019**, *186*, 106070. [[CrossRef](#)]
20. Liu, S.; Papanikolaou, A. Regression analysis of experimental data for added resistance in waves of arbitrary heading and development of a semi-empirical formula. *Ocean Eng.* **2020**, *206*, 107357. [[CrossRef](#)]
21. Abbasnia, A.; Guedes Soares, C. Fully nonlinear and linear ship waves modelling using the potential numerical towing tank and NURBS. *Eng. Anal. Bound. Elem.* **2019**, *103*, 137–144. [[CrossRef](#)]
22. Hou, H.; Krajewski, M.; Ilter, Y.K.; Day, S.; Atlar, M.; Shi, W. An experimental investigation of the impact of retrofitting an underwater stern foil on the resistance and motion. *Ocean Eng.* **2020**, *205*, 107290. [[CrossRef](#)]
23. Daidola, J.C. Effects of Hull and Control Surface Roughness on Ship Maneuvering. In *SNAME Maritime Convention, SNAME-SMC-2019-2004*; SNAME: Tacoma, WA, USA, 2019.
24. Kim, S.; Jung, S.M.; Jung, S.; Shin, H.W.; Hwang, D.S. Sea urchin repelling Tannin—FeIII complex coating for ocean macroalgal afforestation. *Chemosphere* **2021**, *263*, 128276. [[CrossRef](#)]
25. DNV. *Corrosion Protection of Ships*; DNV: Bærum, Norway, 2017.
26. SOLAS. *SOLAS Consolidated Edition 2020*; IMO: London, UK, 2020.
27. Stenson, P.A.; Kidd, B.; Chen, H.L.; Finnie, A.A.; Ramsden, R. Predicting the impact of hull roughness on the frictional resistance of ships. In *Proceedings of the International Conference on Computational and Experimental Marine Hydrodynamics (MARHY 2014)*, Chennai, India, 3–4 December 2014.
28. Smith, F.; Colvin, G. *Magnetic Track*; Patent Application No. 2014/0077.587; Patent and Trademark Office: Washington, DC, USA, 2014.
29. Song, S.; Demirel, Y.K.; Atlar, M.; Dai, S.; Day, S.; Turan, O. Validation of the CFD approach for modelling roughness effect on ship resistance. *Ocean Eng.* **2020**, *200*, 107029. [[CrossRef](#)]
30. Sun, W.; Hu, Q.; Hu, S.; Su, J.; Xu, J.; Wei, J.; Huang, G. Numerical Analysis of Full-Scale Ship Self-Propulsion Performance with Direct Comparison to Statistical Sea Trial Results. *J. Mar. Sci. Eng.* **2020**, *8*, 24. [[CrossRef](#)]

31. Farkas, A.; Song, S.; Degiuli, N.; Martić, I.; Demirel, Y.K. Impact of biofilm on the ship propulsion characteristics and the speed reduction. *Ocean Eng.* **2020**, *199*, 107033. [CrossRef]
32. Farkas, A.; Degiuli, N.; Martić, I.; Dejhalla, R. Impact of Hard Fouling on the Ship Performance of Different Ship Forms. *J. Mar. Sci. Eng.* **2020**, *8*, 748. [CrossRef]
33. Ravenna, R.; Song, S.; Shi, W.; Sant, T.; De Marco Muscat-Fenech, C.; Tezdogan, T.; Demirel, Y.K. CFD analysis of the effect of heterogeneous hull roughness on ship resistance. *Ocean Eng.* **2022**, *258*, 111733. [CrossRef]
34. Mikkelsen, H.; Walther, J.H. Effect of roughness in full-scale validation of a CFD model of self-propelled ships. *Appl. Ocean Res.* **2020**, *99*, 102162. [CrossRef]
35. Islam, H.; Ventura, M.; Guedes Soares, C.; Tadros, M.; Abdelwahab, H.S. Comparison between empirical and CFD based methods for ship resistance and power prediction. In *Trends in Maritime Technology and Engineering*; Guedes Soares, C., Santos, T.A., Eds.; Taylor & Francis Group: London, UK, 2022; pp. 347–357.
36. Orych, M.; Werner, S.; Larsson, L. Validation of full-scale delivered power CFD simulations. *Ocean Eng.* **2021**, *238*, 109654. [CrossRef]
37. García, S.; Trueba, A.; Boullosa-Falces, D.; Islam, H.; Guedes Soares, C. Predicting ship frictional resistance due to biofouling using Reynolds-averaged Navier-Stokes simulations. *Appl. Ocean Res.* **2020**, *101*, 102203. [CrossRef]
38. Song, S.; Demirel, Y.K.; Atlar, M. An Investigation Into the Effect of Biofouling on Full-Scale Propeller Performance Using CFD. In Proceedings of the 38th International Conference on Ocean, Offshore & Arctic Engineering (OMAE 2019), Glasgow, UK, 9–14 June 2019.
39. Asnaghi, A.; Svennberg, U.; Gustafsson, R.; Bensow, R.E. Propeller tip vortex mitigation by roughness application. *Appl. Ocean Res.* **2021**, *106*, 102449. [CrossRef]
40. Sezen, S.; Uzun, D.; Ozyurt, R.; Turan, O.; Atlar, M. Effect of biofouling roughness on a marine propeller's performance including cavitation and underwater radiated noise (URN). *Appl. Ocean Res.* **2021**, *107*, 102491. [CrossRef]
41. Carchen, A.; Atlar, M. Four KPIs for the assessment of biofouling effect on ship performance. *Ocean Eng.* **2020**, *217*, 107971. [CrossRef]
42. HydroComp. NavCad: Reliable and Confident Performance Prediction. HydroComp Inc. Available online: <https://www.hydrocompinc.com/solutions/navcad/> (accessed on 30 January 2019).
43. Tadros, M.; Ventura, M.; Guedes Soares, C. Design of Propeller Series Optimizing Fuel Consumption and Propeller Efficiency. *J. Mar. Sci. Eng.* **2021**, *9*, 1226. [CrossRef]
44. Tadros, M.; Ventura, M.; Guedes Soares, C. Optimization procedures for a twin controllable pitch propeller of a ROPAX ship at minimum fuel consumption. *J. Mar. Eng. Technol.* **2022**, 1–9. [CrossRef]
45. Tadros, M.; Ventura, M.; Guedes Soares, C. Towards Fuel Consumption Reduction Based on the Optimum Contra-Rotating Propeller. *J. Mar. Sci. Eng.* **2022**, *10*, 1657. [CrossRef]
46. Tadros, M.; Vettor, R.; Ventura, M.; Guedes Soares, C. Assessment of Ship Fuel Consumption for Different Hull Roughness in Realistic Weather Conditions. *J. Mar. Sci. Eng.* **2022**, *10*, 1891. [CrossRef]
47. ITTC. 1978 ITTC Performance Prediction Method. In Proceedings of the 28th ITTC, Wuxi, China, 17–22 September 2017.
48. ITTC. Skin Friction and Turbulence Stimulation. In Proceedings of the 8th ITTC, Madrid, Spain, 15–23 September 1957.
49. MAN Diesel & Turbo. *32/44CR Project Guide—Marine Four-Stroke Diesel Engines Compliant with IMO Tier II*; MAN Diesel & Turbo: Augsburg, Germany, 2017.
50. Tadros, M.; Ventura, M.; Guedes Soares, C. Optimization procedure to minimize fuel consumption of a four-stroke marine turbocharged diesel engine. *Energy* **2019**, *168*, 897–908. [CrossRef]
51. Tadros, M.; Ventura, M.; Guedes Soares, C. Data Driven In-Cylinder Pressure Diagram Based Optimization Procedure. *J. Mar. Sci. Eng.* **2020**, *8*, 294. [CrossRef]
52. Tadros, M.; Ventura, M.; Guedes Soares, C. Simulation of the performance of marine Genset based on double-Wiebe function. In *Sustainable Development and Innovations in Marine Technologies*; Georgiev, P., Guedes Soares, C., Eds.; Taylor & Francis Group: London, UK, 2020; pp. 292–299.
53. Tadros, M.; Ventura, M.; Guedes Soares, C. Surrogate models of the performance and exhaust emissions of marine diesel engines for ship conceptual design. In *Maritime Transportation and Harvesting of Sea Resources*; Guedes Soares, C., Teixeira, A.P., Eds.; Taylor & Francis Group: London, UK, 2018; pp. 105–112.
54. Tadros, M.; Ventura, M.; Guedes Soares, C. Optimization of the performance of marine diesel engines to minimize the formation of SOx emissions. *J. Mar. Sci. Appl.* **2020**, *19*, 473–484. [CrossRef]
55. Tadros, M.; Vettor, R.; Ventura, M.; Guedes Soares, C. Effect of different speed reduction strategies on ship fuel consumption in realistic weather conditions. In *Trends in Maritime Technology and Engineering*; Guedes Soares, C., Santos, T.A., Eds.; Taylor & Francis Group: London, UK, 2022; pp. 553–561.
56. Tadros, M.; Vettor, R.; Ventura, M.; Guedes Soares, C. Coupled Engine-Propeller Selection Procedure to Minimize Fuel Consumption at a Specified Speed. *J. Mar. Sci. Eng.* **2021**, *9*, 59. [CrossRef]
57. Holtrop, J. A statistical re-analysis of resistance and propulsion data. *Int. Shipbuild. Prog.* **1984**, *31*, 272–276.
58. Holtrop, J. A Statistical Resistance Prediction Method With a Speed Dependent Form Factor. In *Proceedings of Scientific and Methodological Seminar on Ship Hydrodynamics (SMSSH '88)*; Bulgarian Ship Hydrodynamics Centre: Varna, Bulgaria, 1988; pp. 1–7.
59. Holtrop, J.; Mennen, G.G.J. An approximate power prediction method. *Int. Shipbuild. Prog.* **1982**, *29*, 166–170. [CrossRef]

60. Carlton, J. *Marine Propellers and Propulsion*, 2nd ed.; Butterworth-Heinemann: Oxford, UK, 2012.
61. Tadros, M.; Vettor, R.; Ventura, M.; Guedes Soares, C. Effect of propeller cup on the reduction of fuel consumption in realistic weather conditions. *J. Mar. Sci. Eng.* **2022**, *10*, 1039. [[CrossRef](#)]
62. Daidola, J.C. Propeller Roughness and its Effects on Required Freight Rate. In *Sixth International Symposium on Marine Propulsors (smp'19)*; Felli, M., Leotardi, C., Eds.; National Research Council of Italy, Institute of Marine Engineering (CNR-INM): Rome, Italy, 2019.
63. ITTC. Specialist Committee on Surface Treatment—Final report and recommendations to the 26th ITTC. In *Proceedings of the 26th ITTC—Volume II*, Rio de Janeiro, Brazil, 28 August–3 September 2011.
64. Andersson, J.; Oliveira, D.R.; Yeginbayeva, I.; Leer-Andersen, M.; Bensow, R.E. Review and comparison of methods to model ship hull roughness. *Appl. Ocean Res.* **2020**, *99*, 102119. [[CrossRef](#)]
65. MacPherson, D.M. Reliable Propeller Selection for Work Boats and Pleasure Craft: Techniques Using a Personal Computer. In *Proceedings of the SNAME Fourth Biennial Power Boat Symposium*, NJ, USA; 1991.
66. Moreira, L.; Vettor, R.; Guedes Soares, C. Neural Network Approach for Predicting Ship Speed and Fuel Consumption. *J. Mar. Sci. Eng.* **2021**, *9*, 119. [[CrossRef](#)]

Disclaimer/Publisher's Note: The statements, opinions and data contained in all publications are solely those of the individual author(s) and contributor(s) and not of MDPI and/or the editor(s). MDPI and/or the editor(s) disclaim responsibility for any injury to people or property resulting from any ideas, methods, instructions or products referred to in the content.